Hindawi
Geofluids
Volume 2022, Article ID 9426378, 11 pages
https://doi.org/10.1155/2022/9426378

Research Article

Effects of Real-Time High Temperature and Loading Rate on Deformation and Strength Behavior of Granite

YiFeng Zhang, Fan Zhang, Ke Yang, and ZhengYu Cai

School of Civil Engineering, Architecture and Environment, Hubei University of Technology, Wuhan 430068, China

Correspondence should be addressed to Fan Zhang; fanzhang@hbut.edu.cn

Received 16 March 2022; Revised 11 April 2022; Accepted 15 April 2022; Published 14 May 2022

Academic Editor: Zhijie Wen

Copyright © 2022 YiFeng Zhang et al. This is an open access article distributed under the Creative Commons Attribution License, which permits unrestricted use, distribution, and reproduction in any medium, provided the original work is properly cited.

Knowledge of deformation and strength behavior of rocks under high in situ temperature is highly important for the control of geological disasters in exploration of hot dry rock and mining in deep formation. In this study, uniaxial compression tests were carried out on granite under different real-time high-temperature conditions (25, 200, 300, 400, 500, 600, and 700°C) and loading rates (0.01, 0.1, and 0.5 mm/min). The effects of real-time high temperature and loading rate on the uniaxial compressive strength and elastic modulus of granite were studied, and the microscopic morphology of the fracture surface was analyzed. The results show that the uniaxial compressive strength and elastic modulus of granite increase first and then decrease with the increase of temperature. The uniaxial compressive strength clearly increases at 200°C and decreases gradually when the temperature exceeds 300°C. Under the same temperature conditions, the uniaxial compressive strength of granite decreases and the elastic modulus increases with increasing loading rate. When the temperature reaches 600°C, the effect of the loading rate on the uniaxial compressive strength and elastic modulus of granite decreases significantly. The test results are compared with the results of work performed on quenched granite. Under real-time high-temperature conditions, the thermal crack effect has a significant influence on the uniaxial compressive strength and elastic modulus of granite, without the thermal hardening effect of quenched granite. During hydraulic fracturing, the rock skeleton near the injection well is cooled and shrunk, as is the thermal hardening effect caused by high-temperature quenching. The formation of thermal equilibrium leads to the large-scale extension of fracture cracks along the weak plane structure, such as the effect of thermal cracks on granite under real-time high-temperature conditions.

1. Introduction

Hot dry rock (HDR) energy is a well-recognized clean and renewable green energy which has many advantages, such as stability and safety, high utilization rate, and low operating cost [1]. HDR is widely distributed in the granite at depths in the order of 5 to 6 km, temperatures varying from 150 to 650°C [2, 3]. At present, HDR development is mainly concentrated in the granite thermal reservoir. Therefore, it is important to investigate the effect of real-time high temperature on the physical properties and mechanical behavior of granite for the design, construction, and maintenance of enhanced geothermal system (EGS).

A large number of experimental studies have been performed to investigate the physical properties and mechanical behavior of rocks subjected to thermal treatment. Zhang et al. [4] investigated the changes in the physical behavior of granite and sandstone after heat treatment by the uniaxial compression test and showed that the loss of adhered water, bound water, and structural water has a great influence on the mechanical properties of rocks at high temperature. Wang et al. [5] investigated the acoustic emission (AE) characteristics of granite during uniaxial compression tests after thermal treatment, and the experimental results showed that AE energy increases with the increase of treatment temperature. Chen et al. [6] measured the macroscopic mechanical properties of granite using uniaxial compression test after high-temperature thermal treatment and found that the uniaxial compressive strength gradually decreases with increasing temperature. Liu et al. [7] studied the mechanical properties of granite after high-temperature thermal treatment by the uniaxial compression test, and the results

showed that 600°C is the critical temperature of granite. Zhao et al. [8] and Sun et al. [9] found that high temperature causes prefabricated cracks in granite to continue to expand and even produce new cracks. As the temperatures increase, the number and width of the microcrack increase, and the granite transforms from brittle to ductile. David et al. [10] analyzed the relation of the evolution of the physical properties and the amount of damage induced and indicated that changes in mineral composition and fracture size are the reasons for the decline of granite strength. Heuze [11] studied the influence of the thermal expansion coefficient and the thermal diffusivity on the mechanical properties of granite. Chaki et al. [12] confirmed the strong influence of thermal damage on physical properties of granite and determined parameters for the characterization of connected porosity and overall damage.

Furthermore, the thermal stimulation method can be effectively utilized to improve flow performance in tight porous media with an induced thermal shock by inducing the thermal gradient for permeable cracks, thus achieving geothermal reservoir stimulation [13]. Kumari et al. [13, 14] conducted strength tests under unconfined conditions, Brazilian tensile strength tests, and permeability tests in quenched granite. The results showed that increasing temperature causes significant reductions in the permeability of granite due to the thermally induced volumetric expansion. The failure mechanism of granite transitions from a brittle to a quasibrittle state. Zhang et al. [15] studied the damage variables and pores of granite after thermal shock, and the results showed that thermal shock induced by rapid cooling can cause more damage to granite than that induced by slow cooling, leading to a larger size and number of internal pores. Weng et al. [16] utilized integrated acoustic emission (AE) and digital image correlation (DIC) techniques to study the micro/macrocracking characteristics of the granite sample upon different heating/cooling cycles. The results showed that surface cracks and internal microcracks (including intergranular and intragranular) in granite increase significantly with the number of heating/cooling cycles. Li et al. [17] observed the generation of granite cracks in the process of hydraulic fracturing using AE and indicated that the coalescence of microcracks is a key precursor to hydraulically induced cracking. Avanthi Isaka et al. [18] comprehensively investigated the influence of heating followed by cooling on the alteration of microstructural properties of granite. The analysis revealed considerable unstable deterioration of quartz and feldspar grains subjected to thermal stresses, while biotite minerals show the most stable behavior against thermal shock-induced microcracking. Shao et al. [19] studied the effect of the cooling rate on the mechanical behavior of heated granite through uniaxial compression tests, and the results showed that thermal cracks during the cooling treatment of the heated sample for higher temperatures are the main reason for the decrease of the mechanical characteristics.

Thermal cracking behavior of granite at high temperature and high pressure is the key to the performance of HDR geothermal energy extraction system. Yang et al. [20] evaluated the influence of thermal effect on strength and deformation behavior, and the results showed that crack damage and maximum axial deformation gradually increase with increasing temperature. Gautama et al. [21] measured the thermal physical properties of granite in the range of 25 to 250°C and found that the thermal expansion coefficient of granite increases with the increase of temperature, while the thermal conductivity, thermal diffusivity, and elastic wave velocity of granite decrease gradually with increasing temperature. Gu et al. [22] explored the mechanical properties of granite under heating conditions, and indicated that the ability of the rock to resist deformation gradually weakens under the effect of temperature. Zhao et al. [23] conducted permeability tests on granite at high temperature and high pressure, and the results showed that thermal cracks in granite are induced by intragranular and intergranular thermal stress, and the critical temperature of permeability change decreases with increasing confining pressure. Yin et al. [24] performed triaxial compression tests on granite at high temperature, and the results showed that the larger crystal particles and the extreme heterogeneity of the coarse-grained granite lead to larger thermal deformation and greater deterioration of the mechanical properties. Ranjith et al. [25] carried out the uniaxial compressive tests of sandstone at various temperatures and found that the mineralogical changes in the sandstone cement with heating temperature have a significant influence on changes in mechanical behavior.

The previous work is devoted to rock by investigating the influence of thermal treatment and high-temperature quenching treatments on the macroscopic mechanical properties of rock. The results of experimental studies performed on preheated samples at room temperature are insufficient to represent the essential characteristics of rocks at high temperature in geothermal applications. In addition, the mechanical testing of granite has rarely integrated the coupling effects of real-time high-temperature conditions and loading rates. For this, uniaxial compression tests were carried out under different real-time high-temperature conditions (25, 200, 300, 400, 500, 600, and 700°C) and loading rates (0.01, 0.1, and 0.5 mm/min). The present study investigated the coupled high in situ temperature and loading rate effects. Then, the effect of real-time high temperature on the thermal damage characteristics of granite was analyzed using scanning electron microscopy (SEM). These comprehensive experimental studies provided knowledge of the underlying mechanisms of thermally induced damage in the geothermal reservoir rocks. The results of the testing were compared to results obtained for similar work carried out on quenched granite, which highlights the variability in the response of granite to real-time high temperatures. The research results could be of great significance for understanding the thermal damage and mechanical behavior of HDR mining.

2. Test Preparation and Process

2.1. Rock Description and Sample Preparation. For the present study, granite samples were collected from Miluo Village of Hunan Province, China. Initial granite samples are uniform and complete, with uniform texture, and no visible

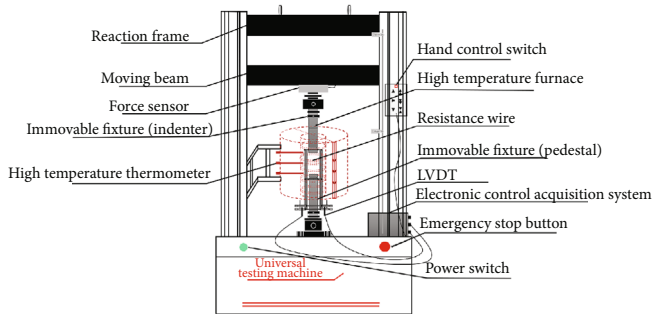

Figure 1: Microcomputer-controlled electronic universal testing machine.

defects were observed on the rock surface. The dimensions of the samples are 38 mm in diameter and 76 mm in length. The surface was polished smooth, and the height, diameter, and flatness all met the requirements. The parallelism was controlled within ±0.05 mm and the surface flatness was controlled within ±0.02 mm, which satisfied the standards of the International Society of Rock Mechanics and Rock Engineering (ISRM) [26]. The natural density and porosity of granite samples are 2.62 g/cm^3 and 0.92%, respectively. The mineral compositions were analyzed by X-ray diffraction, and the results show that the main mineral components are albite (34%), biotite (31%), potash feldspar (21%), quartz (13%), and plagioclase (1%).

2.2. Experimental Equipment and Testing Procedure. In this study, a computer-controlled universal testing machine was used to study real-time high-temperature uniaxial compression tests of granite. As shown in Figure 1, the test equipment is composed of a reaction frame, a high-temperature fixture, a high-temperature furnace, and two displacement sensors (LVDTs). The reaction frame is made of alloy steel and the system has an axial force capacity of 300 kN, which can ensure that the overall stiffness of the testing machine meets the test requirements. The high-temperature fixture is located in the high-temperature furnace with the maximum heating temperature of 1200°C. The granite sample was placed in the center of the high-temperature fixture to ensure that the center of the sample was under pressure. Granite samples were heated in the furnace at atmospheric pressure with a rate of 5°C/min until the prescribed temperature was reached. The heating temperature was held for 2 h to achieve stabilization of the temperature throughout the samples, in order to reduce the effect of the thermal gradient inside the samples and to ensure that the cracking process was induced merely by the temperature effect. Uniaxial compression tests of granite were carried out under the condition of constant target temperature. The granite sample was loaded using the displacement control method. The axial strain was measured by two displacement sensors (LVDTs). The difference between the two displacement sensor (LVDTs) measurements was not significant. This difference was mainly attributed toward that the sample was not completely parallel to the main direction of the axial stress at the time of installation. Installation errors were eliminated using average values. At least three samples were taken for each working condition to ensure the accuracy of the test.

3. Results and Discussion

3.1. Macroscopic Failure Mode. Figure 2(a) shows the macroscopic failure mode of granite after the uniaxial compression test at real-time high temperature. Granite exhibits an X-shaped conjugate inclined plane shear failure. The angle between the failure surface and the load axis is the conjugate shear fracture angle (β). Figure 2(a) also shows that the granite samples are thorough and serious. The area affected by the end effect of the granite sample has many minor extensile cracks at both ends of the sample and the junction of the shear cracks. The middle of the granite sample presents an X-type shearing fracture along the axial loading direction, and its macroscopic cracks are diagonally through [27, 28]. The damage surface is rough. The granite samples are broken down to a number of little pieces at the end of the tests. As shown in Figure 2(b), with the increase of temperature, the surface color of granite samples gradually changes from gray-blue to gray-white. The main reason for this color change is oxidation of biotite and K-feldspar minerals at high temperature. The obvious oxidation of ferrous compounds of these minerals is found in black mica and potassium feldspar minerals [13, 29, 30].

3.2. Microstructure of Fracture Surface. Figure 3 presents the microcrack morphology of the granite after uniaxial compression test under real-time high-temperature conditions by scanning electron microscope (SEM), and the red dotted line indicates the microcracks. Figure 3 shows that high temperature has a significant effect on the expansion of cracks in granite. At 25°C, a few initial cracks are observed in the fracture plane of the granite sample (Figure 3(a)), indicating that the fracture surface of the granite mineral grains in the initial state, the crystal grains remain in tight contact and have almost complete microstructure. When the temperature increases to 200°C, although a few initial grain boundaries and cracks can be observed, the relatively weak grain boundary cementation produces a small amount of grain boundary cracks with small length and small pore size. Most of the grain boundaries remain undivided in this temperature (Figure 3(b)). Below 300°C, no transgranular cracks occur

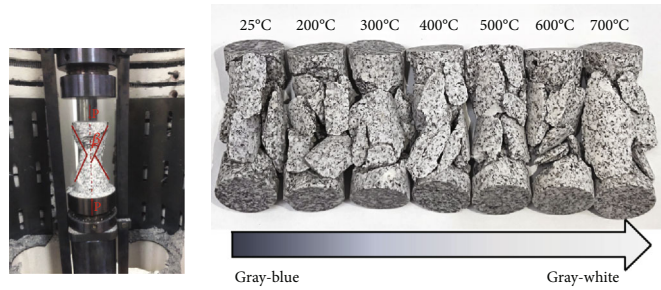

Figure 2: Macroscopic failure morphology of granite samples. (a) Failure morphology of the granite sample in the uniaxial compression test. (b) Color change and failure morphology of granite samples under different real-time high temperatures.

in granite samples [20]. When the temperature exceeds 300°C, the number of grain boundary cracks increases gradually, the length and aperture of grain boundary cracks increase accordingly, and some grain boundary cracks begin to connect. At 400°C, the fracture aperture of intercrystalline cracks increases significantly (Figures 3(c) and 3(d)) [14, 31]. When the real-time temperature is 500°C, the length and width of intracrystalline cracks and intergranular cracks had been increasing as the temperature increases, and the transgranular cracks become increasingly obvious (Figure 3(e)). The quartz undergoes the transition in the crystal structure from α type to β type at 573°C [32]. At temperatures above 600°C, a large number of transgranular cracks appear on the fracture plane, and many crystals are segmented into small cellular structures by transgranular cracks (Figures 3(f) and 3(g)). The internal cracks in granite expand from intergranular cracks to transgranular cracks with the increase of temperature. Further, widely propagated larger cracks arise at the quartz-quartz and quartz-feldspar grain boundaries. The microfracture zone is composed of the main crack and intersecting branch cracks [33, 34]. Under the coupling effect of high temperature and stress, macroscopic cracks are formed, which led to the rapid deterioration of the macroscopic mechanical properties of granite.

3.3. Stress-Strain Curve. The typical stress–strain curves obtained from the real-time high-temperature uniaxial compression tests are shown in Figure 4. Figure 4 also shows that the stress-strain curves of the granite uniaxial compression test under real-time high temperature and different loading rates undergo the compaction stage, the linear elastic stage, the yield stage, and the failure stage [35]. In the initial compaction stage, the curve shows a "downward concave" nonlinear increase under the action of low load, and the microcracks in the granite gradually close under the action of pressure [36, 37]. As the temperature increases, the longer the compaction stage of the stress-strain curve [38–40]. In the linear elastic stage of the stress-strain curve, the microcracks expand stably, and the slope of the curve decreases with the increase of temperature. In granite from the yield phase of the curve to the failure phase of the curve, the granite changes from elastic deformation to plastic deformation with the increase of axial pressure, and the internal fissure expands continuously [41, 42]. In the failure stage, the stress-strain curves display the granite to reach the peak stress and then the stress suddenly decreases. Cracks develop rapidly, forming a macroscopic fracture surface, and the internal structure is destroyed and completely losing the bearing capacity. Between 25 and 500°C, the stress-strain curve shows that the failure mode of the granite is abrupt instability. Granite has typical brittle failure characteristics. The temperature increases from 600 to 700°C, and the plastic properties of granite increases, whereas the brittle properties decrease with increase in temperature. The stress-strain curves have obvious ductile deformation characteristics. For the granite sample, the strain variation increases from the yield point to peak pressure, and the time for the growth of internal cracks to breakdown gets longer. Figure 4 also shows that the process from the yield point to the peak strength is accompanied by an obvious nonlinear behavior. This is due to the high temperature causing the gradual transformation of quartz and feldspar in granite from brittle microcracks to a wider fragmented flow zone. The failure mode of granite becomes from brittle failure to ductile failure and presents the characteristics of semibrittle flow failure [42–44].

3.4. Uniaxial Compressive Strength (UCS). As shown in Figure 5, the UCS of granite shows a variation pattern of increasing and then decreasing with the increase of temperature. The UCS of granite increases significantly with increasing temperature from 25 to 200°C. The enhancement of biotite particles is the main reason for the reinforcement in mechanical properties under the effect of high temperature. At the same time, the mineral particles' volume expansion causes intergranular contact compaction, resulting in increased mutual attraction and cohesion between minerals [37, 45]. The UCS decreases continuously with increasing temperature between 300 and 600°C. This is due to the uneven thermal expansion of the mineral particles with different thermal expansion coefficients in granite, leading to the continuous expansion of cracks [32]. As the temperature rises, the cohesion continues to decrease [45]. Furthermore, the loss of adhered water, bound water, and structural water leads to the damage of mineral crystalline structure [46, 47]. At 573°C, the α-type to β-type transition

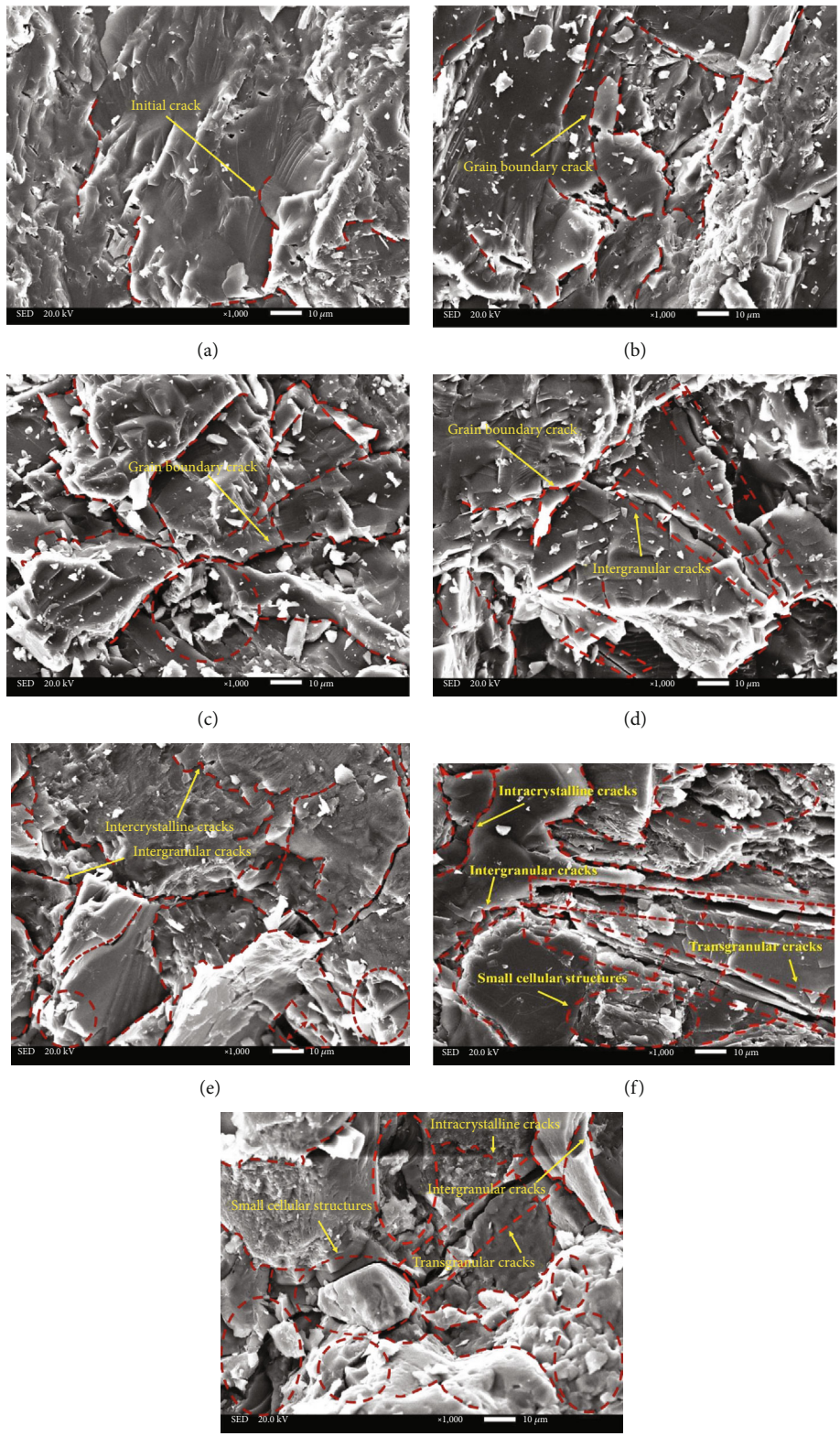

Figure 3: SEM images of the granite fracture surface at different real-time high temperatures: (a) 25°C; (b) 200°C; (c) 300°C; (d) 400°C; (e) 500°C; (f) 600°C; (g) 700°C.

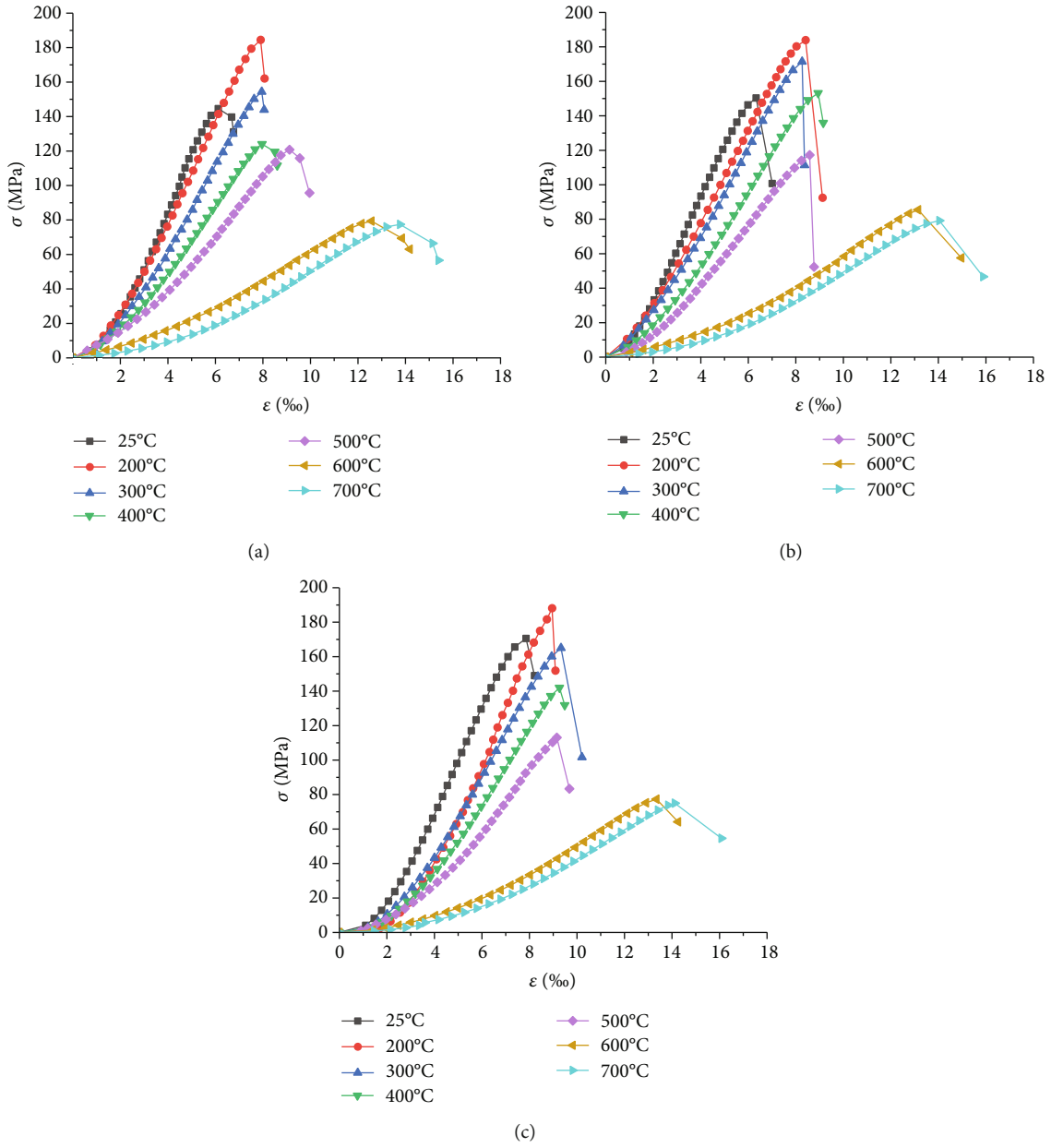

Figure 4: Stress-strain curves of granite under uniaxial compression at real-time high temperature: (a) 0.01 mm/min; (b) 0.1 mm/min; (c) 0.5 mm/min.

in the quartz crystal structure leads to microstructural rearrangement [48]. The extension of the crack in the quartz region increases significantly, forming a good crack network, leading to a rapid increase in structural failure [12, 49, 50]. Above 600°C, the number of cracks remains constant, without forming new cracks, and the length and width of the cracks gradually increase with continuous loading of the axial load [40]. The UCS of granite shows a slight decrease.

As shown in Figure 5, the UCS of granite for three different loading rates (0.01, 0.1, and 0.5 mm/min) shows the similar general trend with increasing temperature. The UCS of granite hardly changes with increasing loading rate, indicating that loading rate has not significantly influenced granite strength [33]. Compared to the other two loading rates (0.01 and 0.1 mm/min), at the loading rate of 0.5 mm/min, the UCS of granite is greater from 25 to 200°C, and the UCS is smaller in the range of 200 to 600°C. Between 600 and 700°C, a similar decreasing trend of UCS is observed for all three loading rates of granite. Under the loading rate of 0.5 mm/min, the UCS increases in the range of 25 to 200°C, which is due to the fact that the distance between individual mineral interfaces decreases more rapidly, resulting in the increase of cohesion. When the temperature exceeds 300°C, the higher the loading rate, the stronger the sliding of the various mineral particles, and the faster the

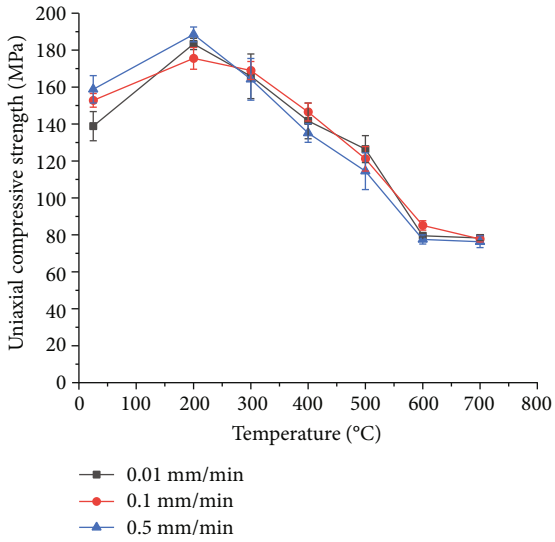

Figure 5: Relationship curves between uniaxial compression strength and temperature of granite under real-time high temperature.

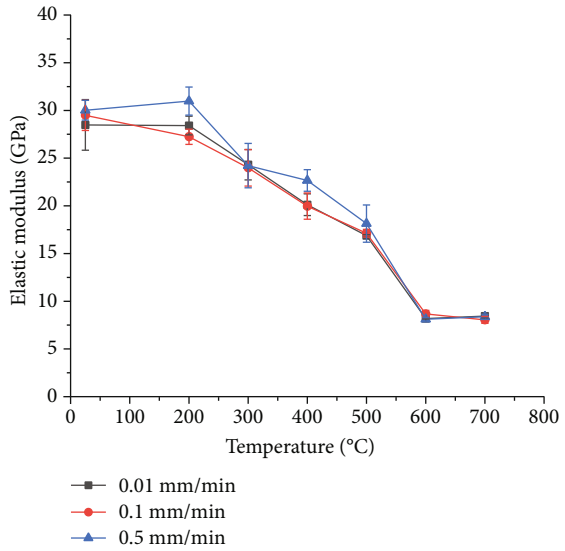

Figure 6: Relationship curves between elastic modulus and temperature of granite under real-time high temperature.

crack expansion produces secondary cracks and branches of the crack, accelerating the formation of internal defects [51]. As shown in Figures 3(d)–3(g), the length and width of intracrystalline and intercrystalline cracks in the granite increase greatly as the temperature increases from 400 to 700°C [52]. At 600°C, the amount of quartz has a significant effect on thermally induced microcracks due to the particularity of its thermal expansibility. Microcracks are growing into one other, creating a mesh of microcracks. Between 600 and 700°C, the brittle to plastic transition of granite occurs within this temperature range. Ductile properties dominate granite damage at high temperatures [53]. The increase in the loading rate has no obvious effect on crack propagation [54], and the UCS is almost unchanged.

3.5. Elastic Modulus. In this study, the tangent modulus in the elastic region of the stress–strain curve (approximately 40 to 60% of the peak strength in the experiments) is defined as the elastic modulus [22]. As shown in Figure 6, the elastic modulus of granite under real-time high temperature shows an overall decreasing trend with increasing temperature. In the range of 25 to 200°C, the mineral particles of granite are compacted, the microstructure is slightly damaged, and the elastic modulus hardly changes. The elastic modulus gradually decreases when the temperature is between 300 and 500°C, and the trend of the elastic modulus is similar to the trend of the UCS. When the temperature exceeds 600°C, microcracks are growing into one other, creating a mesh of microcracks, and the porosity continue to increase, resulting in no significant change in elastic modulus [30, 54].

Figure 6 shows that the elastic modulus variation with increasing temperature follows the similar tendency for all three different loading rates (0.01, 0.1, and 0.5 mm/min) of granites. Under the loading rate of 0.5 mm/min, the elastic modulus of granite increases in general. In the range of 25

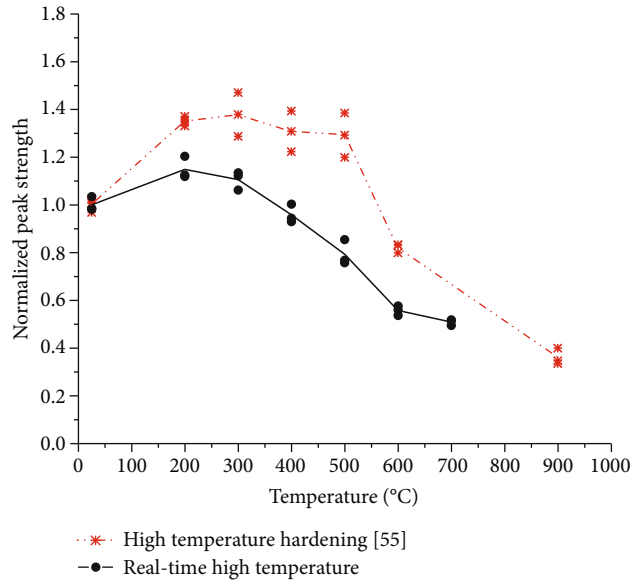

Figure 7: Normalized peak strength versus test temperature curves for granite at real-time high temperature and granite after high-temperature quenching.

to 500°C, the cracks in granite dominated by axial load have a lower degree of expansion and fewer numbers than those under low loading rate, resulting in an overall increase of elastic modulus. When the temperature exceeds 600°C, the increase in the loading rate has no effect on the elastic modulus.

4. Further Discussions

4.1. Comparison of Mechanical Properties of Real-Time High-Temperature Granite and Quenched Granite. Figure 7 shows

the trend of normalized peak strength versus test temperature curves for granite at real-time high temperature and granite after high-temperature quenching. Between 25 and 200°C, the UCS of granite samples increases significantly with the increase of temperature. Between 200 and 500°C, the UCS decreases greatly with increasing temperature. When the temperature exceeds 600°C, the UCS decreases slightly with increasing temperature. The UCS increases significantly at 200°C. Beyond 300°C, the high temperature leads to uneven thermal expansion of the mineral particles and the thermal cracks gradually expand with increasing temperature [9]. At this time, the thermal crack creation has a significant effect on the UCS of granite samples. Compared with the granite samples after high-temperature quenching, there is no uneven stress field and cooling shrinkage [55]. Due to the propagation of the thermal cracks, the internal microstructure of granite is destroyed, leading to a gradual decrease in the UCS of granite samples within the temperature range of 300 to 500°C. Beyond 600°C, the UCS of granite samples decreases under real-time high-temperature conditions. This can be attributed toward the absence of thermal hardening effect in the granite, which results in a higher degree of crack expansion and a larger number of cracks [56], and the UCS decreases more clearly. After high-temperature quenching, the UCS of granite samples increases from 25 to 500°C. The UCS decreases significantly after the temperature reaches 500°C. Between 25 and 500°C, the strength of the outer surface of quenched granite increases rapidly, while the mineral particles do not cool synchronously with the outer surface of quenched granite. The strong temperature gradient results in high local thermal stress, resulting in the nonuniform local plastic strain field, which inhibits thermal crack propagation. The cohesion of granite samples increases, and the internal shrinkage occurs sharply, which has an obvious thermal hardening effect; the UCS of granite samples increases [15]. Above 500°C, a large number of thermal cracks occur and the cohesion of the material decreases significantly, resulting in a significant decrease in the UCS of granite samples.

Figure 8 shows the trend of normalized elastic modulus versus test temperature curves for granite at real-time high temperature and granite after high-temperature quenching. When the temperature is between 25 and 500°C, the elastic modulus of granite samples decreases greatly with increasing temperature. When the temperature reaches 500°C, the elastic modulus of granite samples decreases slightly under real-time high-temperature condition. The degree of propagation of cracks in granite under real-time high-temperature loading increases with increasing temperature, resulting in the destruction of microstructure and the decrease of elastic modulus. Compared with the granite sample after high-temperature quenching, there is no strong temperature gradient in the sample to inhibit the propagation of thermal crack [19]. The elastic modulus of granite samples after high-temperature quenching is similar to the trend of UCS. It increases rapidly between 25 and 500°C and decreases rapidly when the temperature reaches 500°C.

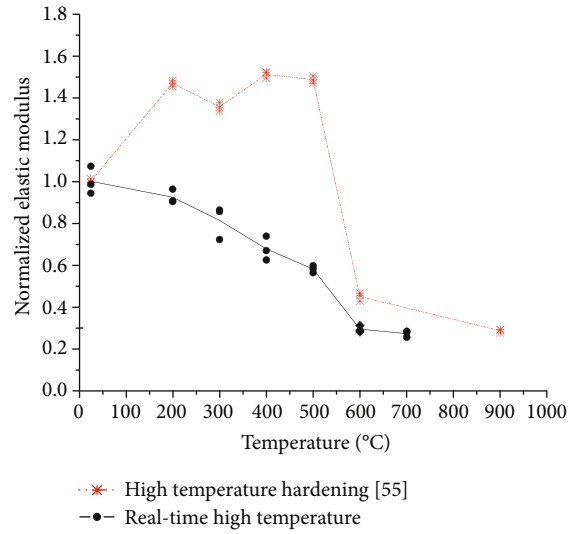

Figure 8: Normalized elastic modulus versus test temperature curves for granite at real-time high temperature and granite after high-temperature quenching.

4.2. Granite Fracturing Mechanism under Real-Time High Temperature. The thermal cracking behavior of granite at high temperature and high pressure is the key to the performance of HDR geothermal reservoir extraction system [23]. During hydraulic fracturing, the fracturing fluid is pumped into the wellbore to increase the pressure at the bottom of the well. With the injection of fracturing fluid, the pressure increases until the rock breaks and produces cracks, as shown in Figure 9(a). At the same time, the injection of fracture fluid causes the solid skeleton to shrink in both transverse and vertical directions. The cooling contraction strain increases over time and remains maximum near the injection well. This phenomenon is similar to the thermal hardening effect of quenched granite [23]. The coupled behavior of real-time high temperature and loading rate is controlled by the characteristic difference between the fluid and the rock matrix. Fluid heat transfer occurs in rock matrix and cracks by convection and conduction. The thermal depletion of the rock matrix is limited to the vicinity of the injection well. As the heat transfer between the fluid and the rock matrix completes, a thermal equilibrium state is formed that causes cracks to continue to grow along the weak interface [57]. Under real-time high-temperature conditions, thermal cracking occurs when the thermal stress exceeds the grain bearing capacity of the granite. Under low-pressure conditions, the difference in the thermal expansion of adjacent minerals is considered to be high-temperature thermal damage to granite. However, under high-temperature and high-pressure conditions, thermal cracking occurs both between adjacent grains (intergranular thermal stress) and within grains (intragranular thermal stress) [52]. According to the microscopic morphology of the granite fracture plane, fractured cracks can extend in a wide range along the weak plane structure, and the weak plane structure can form a natural and efficient water channel. It provides excellent geological conditions for the

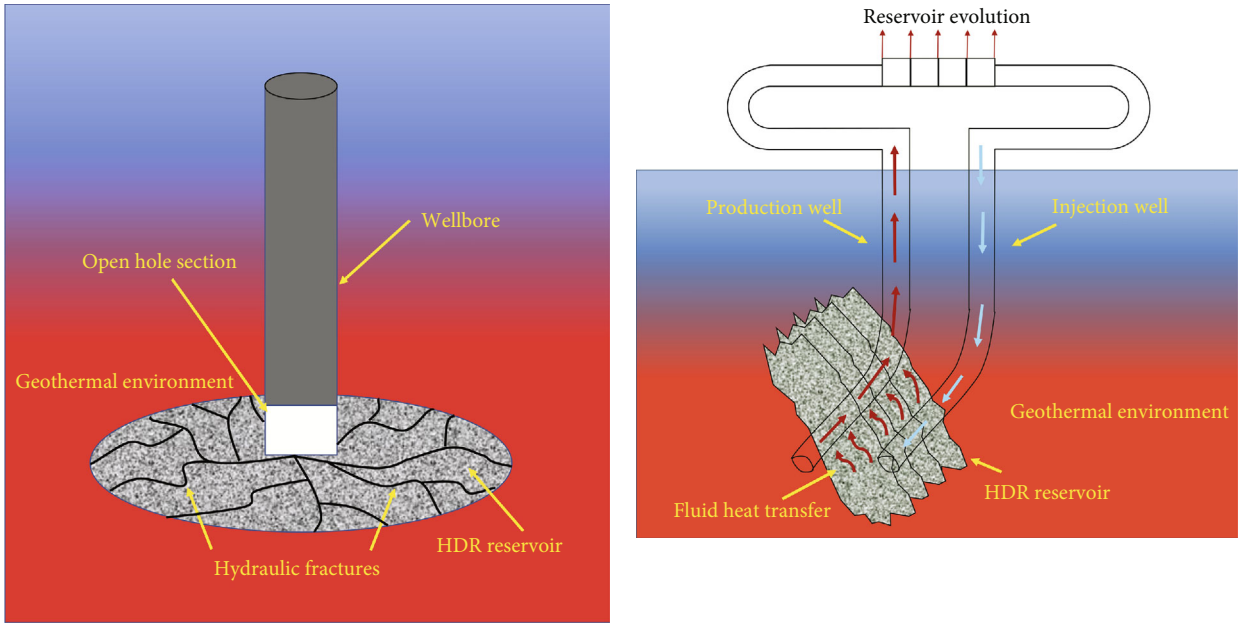

(a) (b)

Figure 9: Granite fracturing mechanism under real-time high-temperature conditions [23, 33]: (a) hydraulic fracturing; (b) fluid heat transfer.

construction of large-volume artificial reservoir and effectively forms large-volume artificial geothermal reservoirs, as shown in Figure 9(b). However, previous studies have shown that the pumping rate during hydraulic fracturing has little effect on the formation of cracks in HDR geothermal formations. The main factors that affect the formation of cracks are geological characteristics such as stress and initial cracks [33]. This is consistent with the effect of the loading rate on the physical and mechanical properties of granite at the real-time high temperature.

5. Conclusions

In this study, uniaxial compression tests were carried out on granite at different real-time high-temperature conditions (25, 200, 300, 400, 500, 600, and 700°C) and loading rates (0.01, 0.1, and 0.5 mm/min). The tests showed that granite has significant thermal damage and mechanical behavior at real-time high temperature. It is found that microcracks occur in granite under real-time high temperature, grain boundary cracks gradually evolve into transgranular cracks, and the extension of microcracks is related to mineral composition and microstructure. The macroscopic cracks formed under the coupling effect of high temperature and stress can lead to rapid deterioration of the macroscopic mechanical behavior of granite. From 25 to 200°C, the UCS and elastic modulus of granite increase significantly. When the temperature is between 200 and 500°C, the thermal cracks continue to expand with increasing temperature, and the UCS and elastic modulus of granite gradually decrease with the increase of temperature. The UCS and the elastic modulus have no obvious changes after 500°C. Compared to the other two loading rates (0.01 and 0.1 mm/min), at the loading rate of 0.5 mm/min, from 25 to 200°C, the UCS and elastic modulus of granite are greater. In the range of 200 to 600°C, the UCS is smaller, and the elastic modulus is greater. Between 600 and 700°C, the UCS and elastic modulus of granite with three loading rates are basically similar. However, the tests showed that the UCS and elastic modulus of granite under real-time high temperature are weakly dependent on the loading rate overall. The results of the testing were compared to results obtained for work carried out on quenched granite; it is found that the UCS and elastic modulus are only affected by the thermal crack.

Data Availability

All the data used to support the findings of this study are included within the article.

Conflicts of Interest

The authors have declared that we have no financial and personal relationships with other people or organizations that can inappropriately influence our work.

Acknowledgments

This work was jointly supported by the National Natural Science Foundation of China (51979100) and Shandong Lunan Geological Engineering Exploration Institute Open Fund (LNY2020-Z08).

References

[1] E. Barbier, "Geothermal energy technology and current status: an overview," *Renewable and Sustainable Energy Reviews*, vol. 6, no. 1-2, pp. 3–65, 2002.

[2] K. Breede, K. Dzebisashvili, X. Liu, and G. Falcone, "A systematic review of enhanced (or engineered) geothermal systems: past, present and future," *Geothermal Energy*, vol. 1, no. 1, p. 4, 2013.

[3] A. C. Gringarten, P. A. Witherspoon, and Y. Ohnishi, "Theory of heat extraction from fractured hot dry rock," *Journal of Geophysical Research*, vol. 80, no. 8, pp. 1120–1124, 1975.

[4] W. Q. Zhang, Q. Sun, S. Q. Hao, J. S. Geng, and C. Lv, "Experimental study on the variation of physical and mechanical properties of rock after high temperature treatment," *Applied Thermal Engineering*, vol. 98, no. 8, pp. 1297–1304, 2016.

[5] Z. L. Wang, A. L. He, G. Y. Shi, and G. X. Mei, "Temperature effect on AE energy characteristics and damage mechanical behaviors of granite," *International Journal of Geomechanics*, vol. 18, no. 3, article 04017163, 2018.

[6] Y. L. Chen, S. R. Wang, J. Ni, R. Azzam, and T. M. Fernández-steeger, "An experimental study of the mechanical properties of granite after high temperature exposure based on mineral characteristics," *Engineering Geology*, vol. 220, pp. 234–242, 2017.

[7] S. Liu and J. Y. Xu, "An experimental study on the physico-mechanical properties of two post-high- temperature rocks," *Engineering Geology*, vol. 185, pp. 63–70, 2015.

[8] Z. H. Zhao, H. R. Xu, J. Wang, X. G. Zhao, M. Cai, and Q. Yang, "Auxetic behavior of Beishan granite after thermal treatment: a microcracking perspective," *Engineering Fracture Mechanics*, vol. 231, article 107017, 2020.

[9] Q. Sun, W. Q. Zhang, L. Xue, Z. Z. Zhang, and T. M. Su, "Thermal damage pattern and thresholds of granite," *Environmental Earth Sciences*, vol. 74, no. 3, pp. 2341–2349, 2015.

[10] C. David, B. Menéndez, and M. Darot, "Influence of stress-induced and thermal cracking on physical properties and microstructure of La Peyratte granite," *International Journal of Rock Mechanics and Mining Sciences*, vol. 36, no. 4, pp. 433–448, 1999.

[11] F. E. Heuze, "High-temperature mechanical, physical and thermal properties of granitic rocks– a review," *International Journal of Rock Mechanics and Mining Sciences & Geomechanics Abstracts*, vol. 20, no. 1, pp. 3–10, 1983.

[12] S. Chaki, M. Takarli, and W. P. Agbodjan, "Influence of thermal damage on physical properties of a granite rock: porosity, permeability and ultrasonic wave evolutions," *Construction and Building Materials*, vol. 22, no. 7, pp. 1456–1461, 2008.

[13] W. G. P. Kumari, P. G. Ranjith, M. S. A. Perera, and B. K. Chen, "Experimental investigation of quenching effect on mechanical, microstructural and flow characteristics of reservoir rocks: thermal stimulation method for geothermal energy extraction," *Journal of Petroleum Science and Engineering*, vol. 162, pp. 419–433, 2018.

[14] W. G. P. Kumari, D. M. Beaumont, P. G. Ranjith, M. S. A. Perera, B. L. Avanthi Isaka, and M. Khandelwal, "An experimental study on tensile characteristics of granite rocks exposed to different high-temperature treatments," *Geomechanics and Geophysics for Geo-Energy and Geo-Resources*, vol. 5, no. 1, pp. 47–64, 2019.

[15] F. Zhang, J. J. Zhao, D. W. Hu, F. Skoczylas, and J. F. Shao, "Laboratory investigation on physical and mechanical properties of granite after heating and water-cooling treatment," *Rock Mechanics and Rock Engineering*, vol. 51, no. 3, pp. 677–694, 2018.

[16] L. Weng, Z. J. Wu, and Q. S. Liu, "Influence of heating/cooling cycles on the micro/macrocracking characteristics of Rucheng granite under unconfined compression," *Bulletin of Engineering Geology and the Environment*, vol. 79, no. 6, 2020.

[17] B. Q. Li, B. Gonçalves da Silva, and H. Einstein, "Laboratory hydraulic fracturing of granite: acoustic emission observations and interpretation," *Engineering Fracture Mechanics*, vol. 209, pp. 200–220, 2019.

[18] B. L. Avanthi Isaka, P. G. Ranjith, T. D. Rathnaweera, M. S. A. Perera, and V. R. S. De Silva, "Quantification of thermally-induced microcracks in granite using X-ray CT imaging and analysis," *Geothermics*, vol. 81, pp. 152–167, 2019.

[19] S. S. Shao, P. L. P. Wasantha, P. G. Ranjith, and B. K. Chen, "Effect of cooling rate on the mechanical behavior of heated Strathbogie granite with different grain sizes," *International Journal Rock Mechanics and Mining Sciences*, vol. 70, pp. 381–387, 2014.

[20] S. Q. Yang, P. G. Ranjith, H. W. Jing, W. L. Tian, and Y. Ju, "An experimental investigation on thermal damage and failure mechanical behavior of granite after exposure to different high temperature treatments," *Geothermics*, vol. 65, pp. 180–197, 2017.

[21] P. K. Gautama, A. K. Verma, T. N. Singh, W. Hu, and K. H. Singh, "Experimental investigations on the thermal properties of Jalore granitic rocks for nuclear waste repository," *Thermochimica Acta*, vol. 681, article 178381, 2019.

[22] B. Gu, Z. Wan, Y. Zhang, Y. Ma, and X. B. Xu, "Influence of real-time heating on mechanical behaviours of rocks," *Advances in Civil Engineering*, vol. 2020, Article ID 8879922, 10 pages, 2020.

[23] Y. S. Zhao, Z. J. Feng, Y. Zhao, and Z. J. Wan, "Experimental investigation on thermal cracking, permeability under HTHP and application for geothermal mining of HDR," *Energy*, vol. 132, pp. 305–314, 2017.

[24] W. T. Yin, Z. J. Feng, and Y. S. Zhao, "Effect of grain size on the mechanical behaviour of granite under high temperature and triaxial stresses," *Rock Mechanics and Rock Engineering*, vol. 54, no. 2, pp. 745–758, 2021.

[25] P. G. Ranjith, R. V. Daniel, B. J. Chen, and M. S. A. Perera, "Transformation plasticity and the effect of temperature on the mechanical behaviour of Hawkesbury sandstone at atmospheric pressure," *Engineering Geology*, vol. 151, pp. 120–127, 2012.

[26] J. A. Franklin, U. W. Vogler, J. Szlavin, and J. M. Edmond, "Suggested methods for determining water content, porosity, density, absorption and related properties and swelling and slake-durability index properties : part 2: suggested methods for determining swelling and slake-durability index properties," *International Journal of Rock Mechanics and Mining Sciences & Geomechanics Abstracts*, vol. 16, no. 2, pp. 151–156, 1979.

[27] J. Liu, E. Y. Wang, D. Z. Song, S. H. Wang, and Y. Niu, "Effect of rock strength on failure mode and mechanical behavior of composite samples," *Arabian Journal of Geosciences*, vol. 8, no. 7, pp. 4527–4539, 2014.

[28] Y. Li, D. Huang, and X. A. Li, "Strain rate dependency of coarse crystal marble under uniaxial compression: strength, deformation and strain energy," *Rock Mechanics and Rock Engineering*, vol. 47, no. 4, pp. 1153–1164, 2013.

[29] M. Hajpal and A. Torok, "Mineralogical and colour changes of quartz sandstones by heat," *Environmental Geology*, vol. 46, no. 3-4, pp. 311–322, 2004.

[30] Z. H. Li, L. N. Y. Wong, and C. I. Teh, "Low cost colorimetry for assessment of fire damage in rock," *Engineering Geology*, vol. 228, pp. 50–60, 2017.

[31] V. G. Ruiz de Argandoña, L. Calleja, and M. Montoto, "Determinacion experimental del umbral de microfisuracion termica de la "roca matriz" o "intact rock"," *Trabajos de geología*, vol. 15, pp. 299–306, 2020.

[32] M. H. B. Nasseri, B. S. A. Tatone, G. Grasselli, and R. P. Young, "Fracture toughness and fracture roughness interrelationship in thermally treated westerly granite," *Pure Applied Geophysics*, vol. 166, no. 5-7, pp. 801–822, 2009.

[33] Z. Zhou, Y. Jin, Y. J. Zeng et al., "Investigation on fracture creation in hot dry rock geothermal formations of China during hydraulic fracturing," *Renewable Energy*, vol. 153, pp. 301–313, 2020.

[34] X. P. Zhou and X. Q. Zhang, "The 3D numerical simulation of damage localization of rocks using general particle dynamics," *Engineering Geology*, vol. 224, pp. 29–42, 2017.

[35] Z. N. Zhu, H. Tian, T. Kempka, G. S. Jiang, B. Dou, and G. Mei, "Mechanical behaviors of granite after thermal treatment under loading and unloading conditions," *Natural Resources Research*, vol. 30, no. 3, pp. 2733–2752, 2021.

[36] Y. J. Zong, L. J. Han, J. J. Wei, and S. Y. Wen, "Mechanical and damage evolution properties of sandstone under triaxial compression," *International Journal of Mining Science and Technology*, vol. 26, no. 4, pp. 601–607, 2016.

[37] R. D. Dwivedi, R. K. Goel, V. V. R. Prasad, and A. Sinha, "Thermo-mechanical properties of Indian and other granites," *International Journal Rock Mechanics and Mining Sciences*, vol. 45, no. 3, pp. 303–315, 2008.

[38] J. B. Walsh, "The effect of cracks on the compressibility of rock," *Journal of Geophysical Research*, vol. 70, no. 2, pp. 381–389, 1965.

[39] E. C. David, N. Brantut, A. Schubnel, and R. W. Zimmerman, "Sliding crack model for nonlinearity and hysteresis in the uniaxial stress- strain curve of rock," *International Journal Rock Mechanics and Mining Sciences*, vol. 52, pp. 9–17, 2012.

[40] L. Griffiths, M. J. Heap, P. Baud, and J. Schmittbuhl, "Quantification of microcrack characteristics and implications for stiffness and strength of granite," *International Journal for Numerical and Analytical Methods in Geomechanics*, vol. 100, pp. 138–150, 2017.

[41] F. Zhang, D. W. Hu, S. Y. Xie, and J. F. Shao, "Influences of temperature and water content on mechanical property of argillite," *European Journal Environmental and Civil Engineering*, vol. 18, no. 2, pp. 173–189, 2014.

[42] X. L. Xu, Z. X. Kang, M. Ji, W. X. Ge, and J. Chen, "Research of microcosmic mechanism of brittle-plastic transition for granite under high temperature," *Procedia Earth and Planetary Science*, vol. 1, no. 1, pp. 432–437, 2009.

[43] E. H. Rutter and K. H. Brodie, "Mechanistic interactions between deformation and metamorphism," *Geological Journal*, vol. 30, no. 3-4, pp. 227–240, 1995.

[44] J. Tullis and R. A. Yund, "Experimental deformation of dry westerly granite," *Journal of Geophysical Research*, vol. 82, no. 36, pp. 5705–5718, 1977.

[45] X. Ma, G. L. Wang, D. W. Hu, Y. G. Liu, H. Zhou, and F. Liu, "Mechanical properties of granite under real-time high temperature and three- dimensional stress," *International Journal Rock Mechanics and Mining Sciences*, vol. 136, article 104521, 2020.

[46] M. Nicco, E. A. Holley, P. Hartlieb, and K. Pfaff, "Textural and mineralogical controls on microwave-induced cracking in granites," *Rock Mechanics and Rock Engineering*, vol. 53, no. 10, pp. 4745–4765, 2020.

[47] K. Burlinson, "An instrument for fluid inclusion decrepitometry and examples of its application," *Rock Mechanics and Rock Engineering*, vol. 111, no. 3, pp. 267–278, 1988.

[48] B. J. Skinner, "Section 6: thermal expansion," in *Handbook of Physical Constants—Revised Edition*, pp. 75–96, The Geological Society of America Memoir, 1966.

[49] P. W. J. Glover, P. Baud, M. Darot et al., "A α/β phase transition in quartz monitored using acoustic emissions," *Geophysical Journal International*, vol. 120, no. 3, pp. 775–782, 1995.

[50] L. F. Fan, J. W. Gao, Z. J. Wu, S. Q. Yang, and G. W. Ma, "An investigation of thermal effects on micro-properties of granite by X-ray CT technique," *Applied Thermal Engineering*, vol. 140, pp. 505–519, 2018.

[51] J. Y. Wu, M. M. Feng, G. S. Han, B. Y. Yao, and X. Y. Ni, "Loading rate and confining pressure effect on dilatancy, acoustic emission, and failure characteristics of fissured rock with two pre-existing flaws," *Comptes Rendus Mecanique*, vol. 347, no. 1, pp. 62–89, 2019.

[52] X. P. Zhou, G. Q. Li, and H. C. Ma, "Real-time experiment investigations on the coupled thermomechanical and cracking behaviors in granite containing three pre-existing fissures," *Engineering Fracture Mechanics*, vol. 224, article 106797, 2019.

[53] S. S. Shao, P. G. Ranjith, P. L. P. Wasantha, and B. K. Chen, "Experimental and numerical studies on the mechanical behaviour of Australian Strathbogie granite at high temperatures: an application to geothermal energy," *Geothermics*, vol. 54, pp. 96–108, 2015.

[54] H. F. Wang, B. P. Bonner, S. R. Carlson, B. J. Kowallis, and H. C. Heard, "Thermal stress cracking in granite," *Journal of Geophysical Research*, vol. 94, no. B2, p. 1745, 1989.

[55] F. Zhang, Y. H. Zhang, Y. Y. Dong, D. W. Hu, and J. F. Shao, "Influence of cooling rate on thermal degradation of physical and mechanical properties of granite," *International Journal of Rock Mechanics and Mining Sciences*, vol. 129, article 104285, 2020.

[56] F. Zhang, Y. H. Zhang, D. W. Hu, and J. F. Shao, "Modification of poroelastic properties in granite by heating–cooling treatment," *Acta Geotechnica*, vol. 16, no. 7, pp. 2165–2173, 2021.

[57] R. Gelet, B. Loret, and N. Khalili, "Thermal recovery from a fractured medium in local thermal non-equilibrium," *International Journal for Numerical and Analytical Methods in Geomechanics*, vol. 37, no. 15, pp. 2471–2501, 2012.